Eur. Phys. J. C 18, 405–416 (2000)
Digital Object Identifier (DOI) 10.1007/s100520000519

THE EUROPEAN PHYSICAL JOURNAL C

Searches for the appearance of ν_τ using neutrino beams from muon storage rings

S. Dutta[1,2,a], R. Gandhi[1,b], B. Mukhopadhyaya[1,c]

[1] Mehta Research Institute, Jhusi, Allahabad, India
[2] S.G.T.B. Khalsa College, University of Delhi, Delhi, India

Received: 4 April 2000 / Revised version: 22 July 2000 /
Published online: 8 December 2000 – © Springer-Verlag 2000

Abstract. We study the possibilities offered by muon storage rings for ν_τ appearance experiments in order to determine masses and mixing angles for the $\nu_\mu \to \nu_\tau$ and $\bar{\nu}_e \to \bar{\nu}_\tau$ oscillations. The dependence of tau event rates on baseline, forward peaking of decay neutrinos with increasing energies, and average fluxes intercepted by detectors of various sizes is discussed. It is found that the baseline length does *not* significantly affect the rates for oscillations of such magnitudes as are suggested by the current atmospheric neutrino data. Subsequently, the effects of cuts on hadronic and wrong sign leptonic modes are computed and used to plot 90% CL contours for the parameter regions that can be explored in such experiments. The results show that even for modest muon beam energies, convincing coverage and verification of the Super Kamiokande parameters is possible. In addition, a very significant enlargement of present day bounds on the mixing parameters for neutrino oscillations of all types is guaranteed by these types of searches.

1 Introduction

The recent results of the Super Kamiokande (Super K) water Cerenkov detector experiment [1] provide firm indications of an anomaly in the flavor ratios and zenith angle dependence of the atmospheric neutrino flux. Although the existence of such an anomaly had already been signalled by earlier data from the Kamiokande [2] and IMB [3] experiments and supported by subsequent Soudan II results [4], the impressive statistical significance of the Super K data has appreciably buttressed its interpretation in terms of neutrino mass and oscillations. This is especially true of the observed zenith angle dependence of the observations, which does not naturally seem to lend itself to any alternative explanation. When combined with results from the CHOOZ reactor experiment [5], analyses [6, 7] of the data tilt the balance towards an interpretation in terms of $\nu_\mu \to \nu_\tau$ oscillations versus other explanations. Evidence that this channel is favored also comes from neutral current event count ratios involving the production of neutral pions measured at Super K [8].

In addition to being the first firm signal for physics beyond the standard model, a determination, even if approximate, of neutrino masses and mixing angles would be a crucial pointer towards the nature of such physics, providing an unprecedented glimpse into what lies beyond our present knowledge of the particle interactions. Thus, the importance of independently verifying the presence of $\nu_\mu \to \nu_\tau$ oscillations can scarcely be overestimated. The firmest confirmation of this hypothesis would be via the detection of τ leptons produced by charged current interactions of ν_τ particles resulting from oscillations of ν_μs. In this paper, we study this possibility in the context of neutrinos obtained from muon storage rings at future muon colliders.

At present, high energy ($\geq$ GeV) neutrino beams for oscillation studies are obtained by allowing charged pions and kaons produced in fixed target accelerator experiments to decay in flight. Recently, however, a new type of neutrino beam, much more intense than those presently available, has been proposed and discussed for neutrino oscillation studies and other neutrino related experiments [9–19]. These beams originate from a high intensity muon source, currently under active design and study as part of an effort to develop a high luminosity muon collider [20]. In addition to the extremely intense and collimated primary neutrino fluxes which will be available from such a source, the beam compositions will be much more precisely known than in those available from pion and kaon decay. A muon storage ring with the straight section pointing towards a neutrino detector situated at a specific baseline length, as described in detail in [12], would lead to a neutrino beam with precisely equal numbers of ν_μ and $\bar{\nu}_e$, or, alternatively, $\bar{\nu}_\mu$ and ν_e, depending on the sign of the parent muons. This is in contrast to the presently available high energy neutrino beams from accelerators, which contain mostly muon neutrinos, but with small con-

[a] e-mail: sukanta@mri.ernet.in
[b] e-mail: raj@mri.ernet.in
[c] e-mail: biswarup@mri.ernet.in

taminations of electron and tau neutrino species. For ν_τ appearance searches, the vastly superior luminosities, absence of contamination and the possibility of higher energies of muon collider neutrino beams make them an attractive proposal which merits further study. Accordingly, we focus here on the physics of tau appearance experiments using neutrinos from muon storage rings, depicting the two flavor oscillation parameter ranges (Δm^2 and $\sin^2 2\theta$) which can be consequently probed in a search for $\nu_\mu \to \nu_\tau$ and $\nu_e \to \nu_\tau$ oscillations[1]. We also present a detailed estimate of how many tau events can be observed in a typical detector as a result of such oscillations, given the constraints and backgrounds involved in the process of detection. Adopting the sample design configuration for muon production, capture, cooling, acceleration and storage prior to decay described in [12], the number of available muons of either sign is $\approx 8 \times 10^{20}$ per year. Of these, one fourth decay in a straight section directed towards the neutrino detector, yielding 2×10^{20} neutrinos and an identical number of anti-neutrinos (ν_μ and $\bar{\nu_e}$, if, for example, the beam consists of μ^-). We use these numbers in all of the following calculations, and refer the reader to [12] for design details leading to the production of the neutrino beams. In Sect. 2 we discuss the broader physics characteristics and dependences of τ production rates at such oscillation experiments. There we also record the conclusion that the expected event rates are largely independent of baseline length, so long as we are investigating oscillations of magnitude suggested by the atmospheric ν_μ data. In Sect. 3 we take up the realistic detection of τ events above backgrounds. Our study includes

(i) $\nu_\mu \to \nu_\tau$ oscillations via charge current production and subsequent decay into hadrons, and
(ii) $\bar{\nu}_e \to \bar{\nu}_\tau$ oscillations via the appearance of wrong sign muons from τ decay to leptonic modes. The specific conventional kT type detector, discussed recently in [12] is considered, and we describe our choices for the kinematic cuts and/or overall detection efficiencies for it.

In Sect. 4 we use the results of the consequent event rate calculations to present 90% CL contours for Δm^2 and $\sin^2 2\theta$ for a variety of muon beam energies and baseline lengths in order to illustrate the extraordinary possibilities offered by muon colliders for studying neutrino oscillations.

2 τ^- appearance event rates using muon collider beams: general characteristics

For the general discussion that this section focuses on, we compute and use the actual $\nu_\tau \to \tau$ charged current (CC) production rates without including experimental cuts to eliminate backgrounds. These are detailed and incorporated later, in Sects. 3 and 4, prior to obtaining contour plots for Δm^2 and $\sin^2 2\theta$. The event rate N_τ (events/kT/year) for τ lepton production from ν_μs subsequent to oscillation is given by

$$N_\tau = 6.023 \times 10^{32} \int \sigma^{\rm CC}_{\nu_\tau} \mathcal{P}_{\nu_{\mu,e}\to\nu_\tau} \frac{{\rm d}\left\langle \Phi_{\nu_\mu} \right\rangle}{{\rm d}E_\nu} {\rm d}E_\nu, \quad (1)$$

where $\sigma^{\rm CC}_{\nu_\tau}$ is the total charged current cross section obtained by integrating (3) below. The oscillation probability between flavors is

$$\mathcal{P}_{\nu_{\mu,e}\to\nu_\tau} = \sin^2 2\theta \sin^2 \left[1.27 \Delta m^2 \frac{L}{E_\nu}\right], \quad (2)$$

with $\Delta m^2 = m^2_{\nu_\tau} - m^2_{\nu_{\mu,e}}$ in eV^2, L = baseline length in km, E_ν being the neutrino energy in GeV, and θ the mixing angle between flavors. $\langle \Phi_{\nu_\mu} \rangle$ is the number of neutrinos in the cone intercepted by the detector averaged over its area. The numerical factor is the number of scatterers (isoscalar nucleons) per kT of the detector material.

We first discuss the cross section, performing our calculation within the renormalization group improved parton model, and focus on the inclusive process $\nu_\tau N \to \tau^- +$ anything, where N is an isoscalar nucleon. On retaining effects of the τ mass[2], the differential cross section can be written in terms of the Bjorken scaling variables $x = Q^2/2M\nu$ and $y = \nu/E_\nu$ as

$$\begin{aligned} \frac{{\rm d}^2\sigma^{\nu,\bar{\nu}}}{{\rm d}x{\rm d}y} = \frac{G_{\rm F}^2 M E_\nu}{\pi} \Bigg[& \left\{ xy + \frac{m_\tau^2}{2ME_\nu} \right\} F_1 + \{(1-y) \\ & - \left(\frac{M}{2E_\nu} xy + \frac{m_\tau^2}{4E_\nu^2} \right) \Bigg\} F_2 \\ & \mp \left\{ xy \left(1 - \frac{1}{2}y\right) - \frac{m_\tau^2}{4ME_\nu} y \right\} F_3 \\ & + \frac{m_\tau^2}{M^2} \left\{ \left(\frac{M}{2E_\nu} xy + \frac{m_\tau^2}{4E_\nu^2} \right) F_4 - \frac{M}{2E_\nu} F_5 \right\} \Bigg]. \end{aligned} \quad (3)$$

Here $-Q^2$ is the invariant momentum transfer between the incident neutrino and outgoing tau, $\nu = E_\nu - E_\tau$ is the energy loss in the lab (target) frame, M and M_W are the nucleon and intermediate boson masses respectively, and $G_{\rm F} = 1.16632 \times 10^{-5}$ GeV^{-2} is the Fermi constant. The limits on x and y are

$$\frac{m_\tau^2}{2M\,(E_\nu - M)} \le x \le 1, \quad A - B \le y \le A + B,$$

where

$$\begin{aligned} A &= \frac{1}{2} \left(1 - \frac{m_\tau^2}{2ME_\nu x} - \frac{m_\tau^2}{2E_\nu^2} \right) \Big/ \left(1 + x \frac{M}{2E_\nu} \right), \\ B &= \frac{1}{2} \left| \left[\left(1 - \frac{m_\tau^2}{2ME_\nu x} \right)^2 - \frac{m_\tau^2}{2E_\nu^2} \right] \right|^{1/2} \Big/ \left(1 + x \frac{M}{2E_\nu} \right). \end{aligned} \quad (4)$$

[1] A full study would involve three flavor oscillations, but our purpose here is to explore the possibilities rather than details, given the fact that muon colliders and neutrino experiments fueled by muons from storage rings are still in the design and development stage; see for instance [20]

[2] Or μ mass, in the case of $\sigma^{\rm CC}_{\nu_\mu}$, which is also calculated below. Clearly, however, the terms proportional to the square of the lepton mass in (3) and (4) are important at the energies of interest for only the τ lepton

Table 1. Analytical expressions for the fits of charge current ν_τ (ν_μ) cross section in picobarns. E_{ν_τ} (E_{ν_μ}) is in units of GeV

	CC Interaction and E_ν Range	Nature of fit	Expression
1.	$\nu_\tau + \mathrm{N} \to \tau^- + X$	cubic	$-9.8656 \times 10^{-8} E_{\nu_\tau}^3 + 2.5523 \times 10^{-5} E_{\nu_\tau}^2$
	20–100 GeV		$+4.1203 \times 10^{-3} E_{\nu_\tau} - 4.4066 \times 10^{-2}$
2.	$\nu_\tau + \mathrm{N} \to \tau^- + X$	linear	$6.6685 \times 10^{-3} E_{\nu_\tau} - 1.1579692 \times 10^{-1}$
	50–2000 GeV		
3.	$\nu_\mu + \mathrm{N} \to \mu^- + X$	cubic	$3.5953 \times 10^{-11} E_{\nu_\mu}^3 - 1.6794 \times 10^{-7} E_{\nu_\mu}^2$
	15–2000 GeV		$+7.0057 \times 10^{-3} E_{\nu_\mu} + 2.6235 \times 10^{-5}$

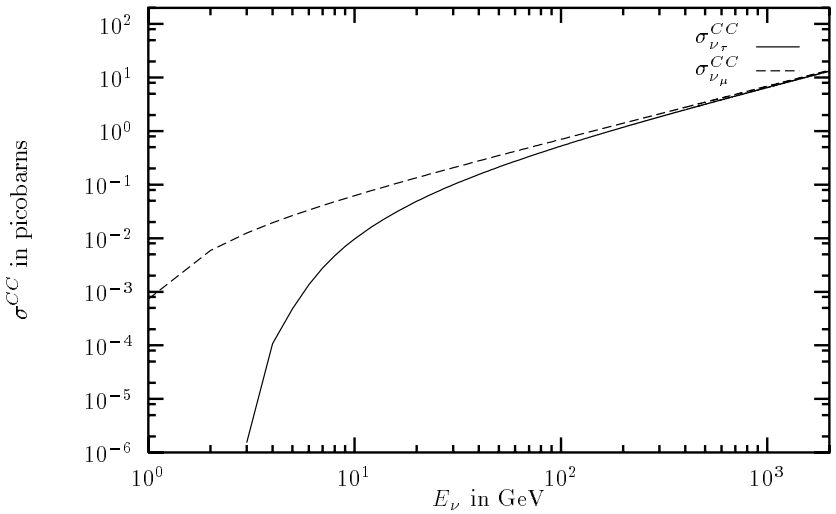

Fig. 1. The CC ν_τ nucleon and ν_μ nucleon scattering cross sections

The F_i are given by

$$
\begin{aligned}
F_2 &= x\left(u + d + \bar{u} + \bar{d} + 2s + 2\bar{b}\right), \\
F_1 &= \frac{F_2}{2x}, \\
F_3 &= \left(u + d - \bar{u} - \bar{d} + 2s - 2\bar{b}\right), \\
F_4 &= \left(-\frac{M\nu}{Q^2}\right)^2 F_2 + \left(-\frac{M\nu}{Q^2}\right) F_1, \\
F_5 &= \frac{F_2}{x}.
\end{aligned}
$$

A straightforward application of the Callan–Gross equations shows that F_4 vanishes in this case. In the above, u, d, c, s and b denote the distributions for the various quark flavors in a proton. For our calculations we use the CTEQ4 parton distributions [21].

Figure 1 shows the total CC cross sections for ν_μ and ν_τ, obtained using the above expressions. For convenience, we give analytic fits for both cross sections in Table 1, over the entire range of energy which is of interest here.

For the calculations of event rates, we assume that the area dimensions of the detector and the baseline length L define a "detection cone" of half angle θ_d with the direction of the muon beam, with detector radius $R_d \equiv L\theta_d$. Thus, for long baselines the choice of θ_d would expectedly be smaller than those for shorter baselines in order to accommodate a realistic detector size. The angular distribution of ν_μ within a chosen detection cone, of course, follows from the decay kinematics of the muon, and is obtained by boosting the familiar distribution of a muon decaying at rest to the requisite beam energy. Figure 2 shows, for various beam energies, the angular distribution $(1/N_{\nu_\mu})\mathrm{d}N_{\nu_\mu}(\theta_p)/\mathrm{d}\theta_p$ in the polar angle θ_p, where $N_{\nu_\mu}(\theta_p)$ is the number of muon neutrinos (prior to any oscillation) contained within a cone of half-angle θ_p, demonstrating the expected forward peaking of muon neutrinos with increasing parent particle energy. This distribution peaks around 1.2×10^{-4} radians for $E_\mu = 500$ GeV, around 3×10^{-4} radians for $E_\mu = 250$ GeV, and even higher for $E_\mu = 50$ and 20 GeV. We remark here that for the wrong sign muon detection mode discussed and used below, the parent $\bar{\nu_e}$ angular distribution differs from the ν_μ distribution shown here, as dictated by decay kinematics.

Next, we note that the oscillation probability in (2) reduces to

$$\mathcal{P}_{\nu_\mu \to \nu_\tau} \simeq 1.27^2 \sin^2 2\theta \Delta m^4 \frac{L^2}{E_\nu^2}, \tag{5}$$

for $\Delta m^2 L/E_\nu \leq 0.1$, and that this condition is satisfied for a significant range of Δm^2 values, even for large baseline lengths, given the high energies contemplated for muon

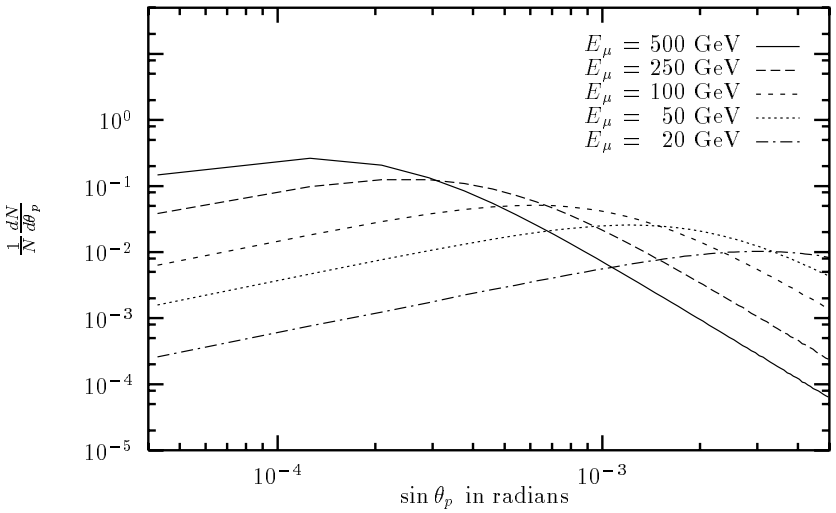

Fig. 2. The angular distribution with polar angle θ_p (angle between the initial muon beam and decaying muon neutrino) for various muon beam energies

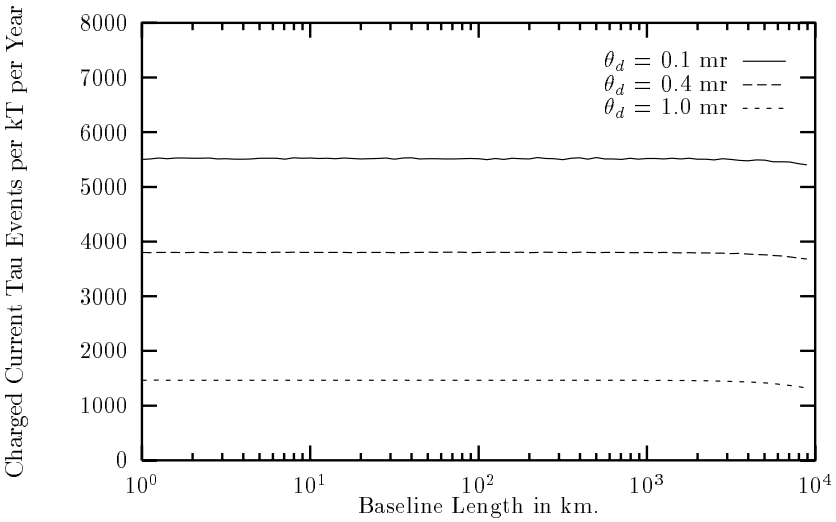

Fig. 3. The insensitivity of the tau event rate to variations in baseline for a fixed detection cone, as discussed in the text. Values of the oscillation parameters are chosen in accordance with the best fits from Super K results

colliders. It is, for instance, valid for the favored value of Super K results, $\Delta m^2 \approx 10^{-3}\,\mathrm{eV}^2$, $\sin^2 2\theta \approx 1$, even for a relatively low 20 GeV muon beam and a 732 km baseline. Since the average flux intercepted by a detector for some fixed θ_d falls as $1/L^2$, from (1) we see that N_τ will be independent of baseline length as long as (5) is satisfied. This independence is illustrated in Fig. 3, where the tau events /kT/yr are plotted versus baseline lengths for three different values of θ_d, for a 250 GeV muon beam energy and $\Delta m^2 = 10^{-3}\,\mathrm{eV}^2$.

Subsequent to oscillation, and when the detector area is taken into account, the enhanced collimation of the neutrinos with increasing beam energy manifests itself in an interesting manner. In general, for a significant part of the range of the energies of interest at muon colliders, $\sigma^{\mathrm{CC}}_{\nu_\tau}$ rises linearly with neutrino energy. For our choice of oscillation parameters, the probability $\mathcal{P}_{\nu_\mu\to\nu_\tau}$ varies with energy as E_ν^{-2} in (5), while the forward peaking of the neutrino beam with energy enhances the flux term as E_ν^2, leading to an overall linear increase in the event rate with energy for a detector of fixed mass whose area matches that of the kinematic decay cone at each energy. In practice, of course, L and R_d (which fix θ_d) and E_μ depend on and are constrained by various factors like geographical location of existing facilities, physics goals, cost and design considerations. It is thus useful to examine the behavior of the τ production event rate when, for instance, L and R_d are fixed and E_μ is varied, with a view to optimization.

In Fig. 4 we plot the tau event rate for $\theta_d = 10^{-3}$ radians, $\Delta m^2 = 2.2 \times 10^{-3}$ eV^2, $\sin^2 2\theta = 1$ and baseline length $L = 732$ km. (The choice of baseline is appropriate to a proposed beam from either CERN to Gran Sasso [22] or from Fermilab to the Soudan laboratory [23].) After the initial rise with energy, it peaks around $E_\mu = 200$ GeV, and then falls and flattens asymptotically with increasing energy. As the position of this peak with respect to E_μ depends on θ_d alone, it will remain invariant under changes of δm^2 and $\sin^2 2\theta$, as long as (5) remains a good approximation.

Figures 5 and 6 compare the yields per kT yr for various detection cones, respectively, as beam energy and Δm^2 are varied. For low beam energies where forward peaking of the decay products is not pronounced, narrower detection cones contain fewer events/kT/yr, but for higher

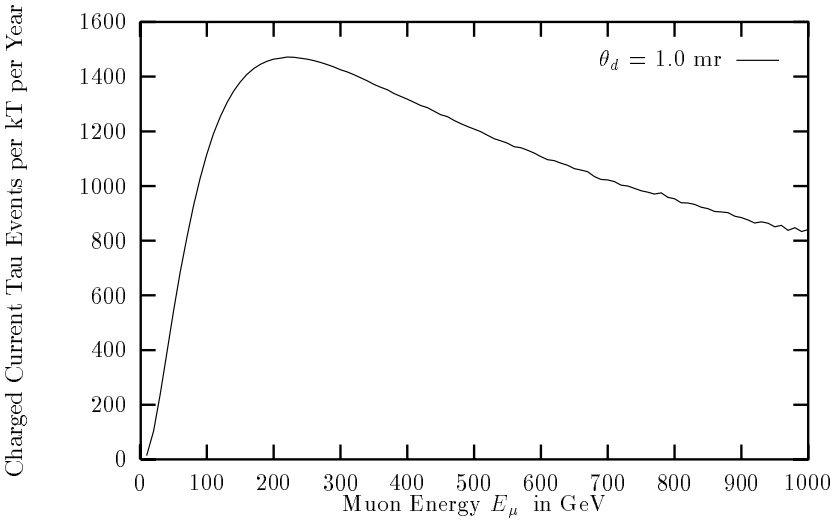

Fig. 4. Variation of tau events with muon beam energy for a baseline length of 732 km and $\Delta m^2 = 0.0022$ and $\sin^2 2\theta = 1$

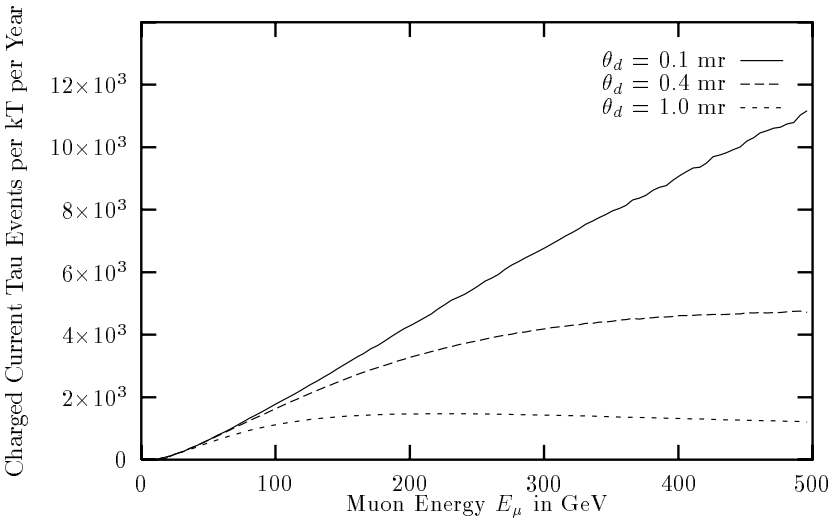

Fig. 5. Variation of tau events for different detection cones with muon beam energy for a given baseline length of 732 km and $\Delta m^2 = 0.0022$ and $\sin^2 2\theta = 1$

energies the behavior is reversed (Fig. 5). For instance, a detector which subtends a $\theta_d = 10^{-4}$ radians cone will see roughly 11 times more events/kT/year for $E_\mu = 500\,\mathrm{GeV}$ than one subtending $\theta_d = 10^{-3}$ radians, since it intercepts a higher average flux $\langle \Phi_{\nu_\mu} \rangle$. The assumption of a uniform flux over the area of the detector can thus be misleading, since the event rate scales very non-linearly with the detector area. In Fig. 6, the rise in the event rate as Δm^4 signalled by (5) and (1) in conjunction is clearly apparent up to Δm^2 values of $O(0.5)\,\mathrm{eV}^2$, after which the sinusoidal behavior sets in.

In conclusion, as illustrated by Figs. 2–6, τ event rates from ν_μ beams at muon colliders have several interesting characteristics which are relevant to experimental design and choice of baseline length and beam energy:

(1) For a substantial and physically interesting range of Δm^2, the event rate (events/kT/year) for a fixed θ_d is to a very good approximation independent of baseline length for a wide range of beam energies (Fig. 3).
(2) For a given choice of say, baseline and detector area (i.e. fixed θ_d), the event rate is maximized at a particular beam energy, independent of the particular values of Δm^2 and $\sin^2 2\theta$ over a considerable portion of their range (Fig. 4).
(3) The intense forward peaking expectedly renders detectors with smaller area superior to those with large area at high beam energies, for a fixed available mass of the detector, and we show the extent to which this affects the actual event rates in Fig. 5.

3 Selection of tau and wrong sign muon events

An important component of any study of the τ appearance due to $\nu_{\mu,e} \to \nu_\tau$ oscillations is the event selection strategy for the τs produced from charged current interactions of the ν_τ. This has been discussed in the literature in the context of several terrestrial experiments that are already in progress [24,25]. Strategies for τ detection have also received consideration in proposals for future experiments [26,27]. For neutrino experiments using a muon storage ring, the detailed prescription for event selection can be formulated only after the detector design is spec-

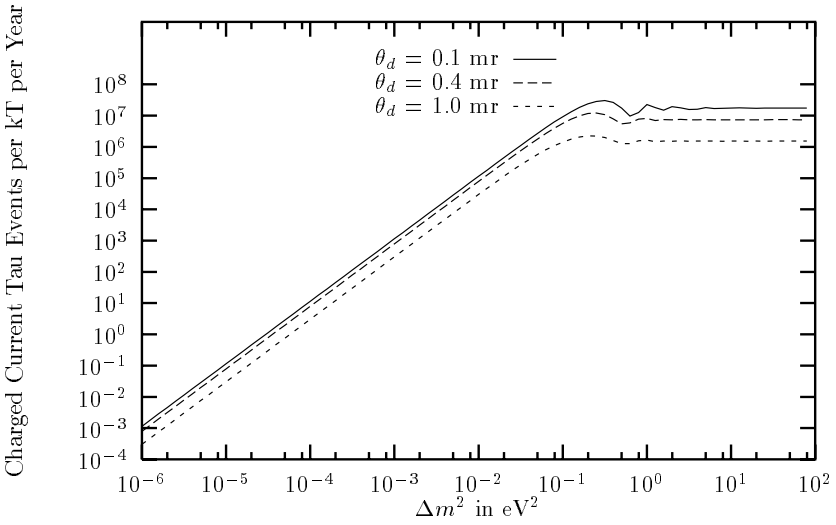

Fig. 6. Variation of tau events for different detection cones with Δm^2 for a muon beam energy of 250 GeV, baseline length of 732 km and $\Delta m^2 = .0022$ and $\sin^2 2\theta = 1$

ified. There are, however, some basic issues concerning the signals and the backgrounds which all experiments are likely to be concerned with. We base our predictions here on these considerations, implemented within a parton-level Monte Carlo calculation. The results presented by us are in connection with a detector of mass 10 kT similar to that described in [12], placed perpendicularly to the muon beam axis, with a short, medium or large baseline, incorporating detailed tracking and particle identification facilities. As can be seen from (1), the event rate N_τ scales linearly with the detector mass for a given θ_d. The precise dependence of $\Delta m^2_{\rm min}$ and $\sin^2 2\theta_{\rm min}$ on various parameters, including beam energy and baseline length, will be discussed in Sect. 4. As can be seen from Figs. 13–18, to be discussed later in the text, more energetic muon beams will be required for probing small values of Δm^2 if one has a detector with smaller mass but similar angular coverage.

We have based our first set of calculations on tau detection through the one-prong hadronic decay channels. This essentially includes the decays $\tau^\pm \to \pi^\pm \nu_\tau$, $\tau^\pm \to \rho^\pm \nu_\tau$ and $\tau^\pm \to {a_1}^\pm \nu_\tau$, with small additional contributions from the K and K^* channels [28]. The $\rho^\pm$ subsequently decays into $\pi^\pm \pi^0$. For the decay of a_1, we have confined ourselves to the mode $\pi^\pm \pi^0 \pi^0$ which leads to a single charged track. The branching ratios into these channels [29] are approximately 11%, 25% and 9% respectively, giving a substantial total branching ratio of about 45%. Thus, essentially one should look for one charged pionic track with 0, 1 or 2 neutral pions in a collinear configuration. The total energy, measured from deposits in the electromagnetic and hadronic calorimeters gives the energy of the $\pi^\pm$, $\rho^\pm$ or ${a_1}^\pm$, which can be combined with the directional information to construct its three-momentum. The backgrounds for signals of this kind (kinks in the charged tracks with missing $p_{\rm T}$) can come, for example, from re-interaction of the hadronic jets coming out of the deep inelastic scattering (DIS) vertex, particularly in the case of neutral current events. Charmed particle production and decays in the DIS processes can also give rise to potential backgrounds. There is also the possibility of muons (from charged current events with no oscillation) being misidentified as pions. And finally, one can have the so-called "white kinks" arising from one-prong nuclear interactions with no heavy ionizing tracks. (These types of kinks usually have a small $p_{\rm T}$, within about 500 MeV for our energy ranges.) With the above considerations in mind, our first set of results (for a 10 kT detector) implements the following event selection criteria for a 250 GeV muon beam [30]:

(1) (1) A minimum $\not{p}_{\rm T}$ of 0.5 GeV;
(2) a minimum energy of 2 GeV for the one-prong decay products from the taus;
(3) A minimum isolation of $\Delta R = 0.7$ between the charged prong from tau decay and the DIS products, where $\Delta R^2 = \Delta\eta^2 + \Delta\phi^2$, $\Delta\eta$ and $\Delta\phi$ being the differences in pseudo-rapidity and azimuthal angle, respectively.

The last criterion ensures that the one-prong charged tracks characteristic of τ decays are at such angles with the beam axis as to set them clearly apart from misidentified muons produced from unoscillated ν_μs as well as from white kinks. At lower (higher) energies, the $\not{p}_{\rm T}$ cut has to be slightly reduced (enhanced) in order to suppress backgrounds with the same effectiveness.

We find that the missing-$p_{\rm T}$ and isolation cuts taken together can remove the entire set of backgrounds due to unoscillated charged current events, whereas the neutral current backgrounds are adequately taken care of by the isolation cuts. Taking everything together, the approximate efficiency of tau detection in our parton-level calculation turns out to be 31% (including the branching ratio for one-prong decays). This is commensurate with the efficiencies expected in, for example, the OPERA experiment [27]. Our second set of results is based on tau appearance due to $\overline{\nu_e}$ oscillating into $\overline{\nu_\tau}$. These will lead to wrong sign muons via charged current interactions. Such signals are relatively background-free; the only significant backgrounds come from charm production at the DIS vertex. For this set for our results we have

(1) a minimum $\not{p}_{\rm T}$ of 0.2 GeV;

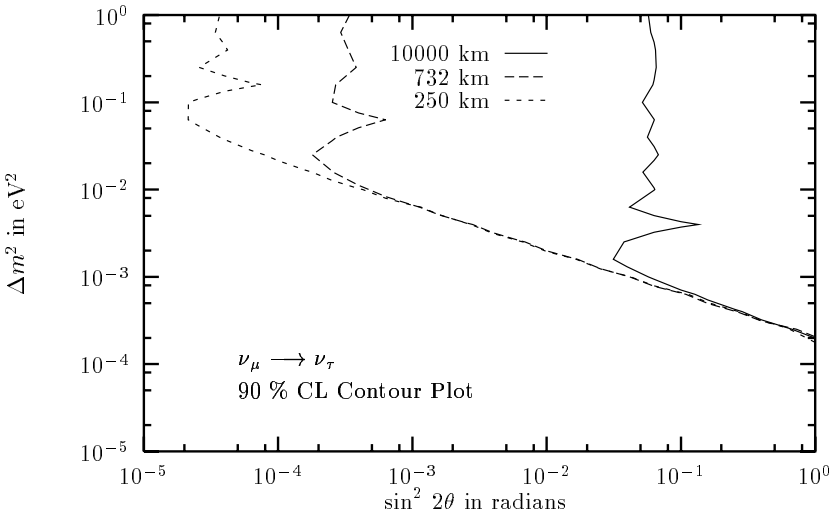

Fig. 7. 90% CL $\nu_\mu \to \nu_\tau$ oscillation contour plot for 20 GeV, 2×10^{20} muons per year with 10 kT target and an angular opening of 0.1 milliradian. τ detection is through one-prong hadronic decay (see text)

(2) a minimum energy of 2 GeV for the wrong sign charged lepton decaying from tau (muon and electron);
(3) A minimum transverse momentum of the wrong sign muon/electron $P_{\rm T}^{\mu,e}$ of 0.2 GeV;
(4) A minimum isolation of $\Delta R = 0.4$ between the wrong sign charged lepton from tau decay and the DIS products.

Finally, although our focus here is on the τ appearance, we also give results in Sect. 4 for the detection of $\overline{\nu_e} \to \overline{\nu_\mu}$ oscillations, detectable again by the presence of wrong sign muons, after implementing suitable cuts.

4 Contours for $\nu_{\mu,e} \to \nu_\tau$ oscillation searches at muon storage rings

In order to demonstrate the possibilities offered by muon storage rings for oscillation studies, we give the corresponding 90% C.L. contours for Δm^2 and $\sin^2 2\theta$ for two flavor mixing. As mentioned earlier, we feel this is adequate at present to obtain a firm feel for the eventual potential of these experiments to comprehensively map the parameter space of neutrino masses and mixing.

Starting with (1) for N_τ, the "bare" events, and folding in the kinematic cuts described above for event selection and background elimination, one obtains N_τ^d, representing the actual candidate events. Requiring $N_\tau^d \leq 2.44$ then delineates the 90% C.L. parameter space. Thus, for each contour the average value of the probability

$$\bar{\mathcal{P}}_{\nu_{\mu,e}\to\nu_\tau} = 2.44/N_\tau^{\rm all}, \tag{6}$$

where $N_\tau^{\rm all}$ is computed from (1) by setting $\mathcal{P}_{\nu_{\mu,e}\to\nu_\tau} = 1$, representing total conversion of the ν_μs to ν_τs, but imposing the cuts as before. Also, we note that [17] for each contour, the reach in Δm^2, i.e. its minimum value, occurring when $\sin^2 2\theta = 1$ is given to a good approximation by

$$\Delta m^2{}_{\rm min} = \left(\frac{2.44}{N_\tau^{\rm all}}\right)^{1/2} \frac{\langle E_\nu \rangle}{L}. \tag{7}$$

Since $N_\tau^{\rm all}$ scales as the product of the flux and the cross section (having the probability term set to 1), it follows that

$$\Delta m^2{}_{\rm min} \propto \langle E_\nu \rangle^{-1/2}. \tag{8}$$

Similarly, the for each contour, i.e. the minimum value of $\sin^2 2\theta$ probed occurs when the other oscillating term in (2) is approximately 1, hence

$$\sin^2 2\theta_{\rm min} \approx \bar{\mathcal{P}}_{\nu_{\mu,e}\to\nu_\tau}. \tag{9}$$

which implies that

$$\sin^2 2\theta_{\rm min} \propto \frac{L^2}{\langle E_\nu \rangle^3}. \tag{10}$$

Finally, the vertical asymptotic part of the contour, occurring when the values of Δm^2 are high enough such that the sine squared term containing it in (2) averages to 1/2 has

$$\sin^2 2\theta = 2\bar{\mathcal{P}}_{\nu_{\mu,e}\to\nu_\tau}. \tag{11}$$

Figures 7, 8, 9 and 10 show contours for τ lepton detection via decay modes containing hadronic final states, for muon beam energies of 20 GeV, 50 GeV, 100 and 250 GeV at 90% C.L. for a 10 kT yr detector, assuming a detection cone of 0.1 milliradians. Each figure has contours for three different baselines, 250 km (Kamioka to KEK), 732 km (CERN to Gran Sasso or Fermilab to Soudan) and 10 000 km (Fermilab to Japan). Figures 11, 12 and 13 show curves for the same choices of baselines and other parameters, but for energies of 50 GeV, 100 GeV and 250 GeV and for the wrong sign lepton detection for $\bar{\nu_e} \to \bar{\nu_\tau}$ oscillation. For a muon beam energy of 20 GeV, no wrong sign muon events survive our (conservative) cuts.

In the regions corresponding to small mass squared differences, all the contours for a given energy tend to merge. This again demonstrates the insensitivity to the baseline in these regions. The scaling relation for $\sin^2\theta_{\rm min}$ with length (for a fixed beam energy) (see (10)) is also reproduced well in the contours. Once one compares different energies, however, the scaling is distorted by the presence

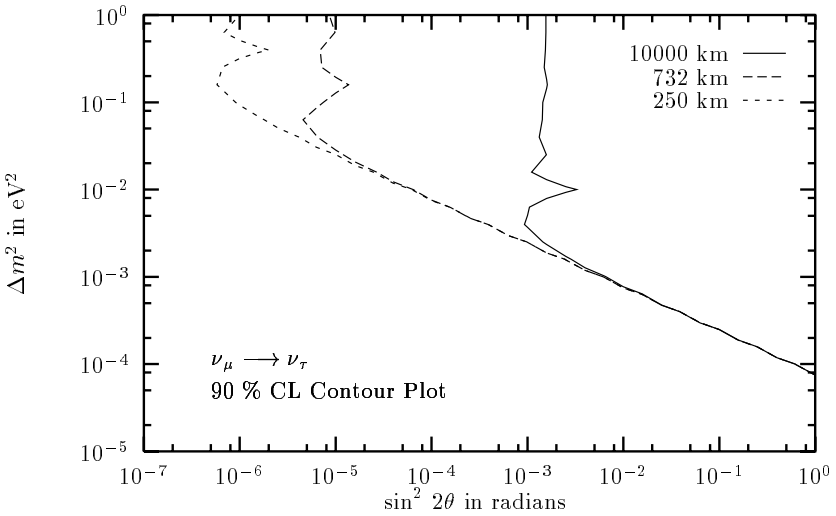

Fig. 8. 90% CL $\nu_\mu \rightarrow \nu_\tau$ oscillation contour plot for 50 GeV, 2×10^{20} muons per year with 10 kT target and an angular opening of 0.1 milliradian. τ detection is through one-prong hadronic decay. (see text)

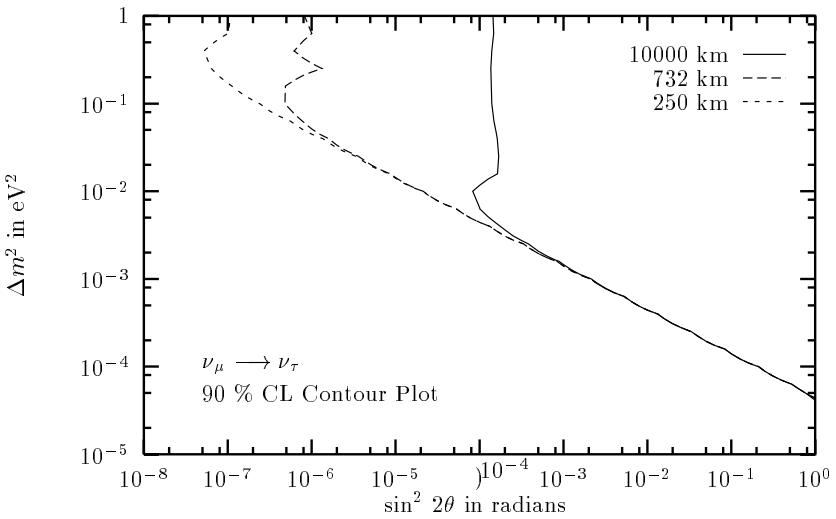

Fig. 9. 90% CL $\nu_\mu \rightarrow \nu_\tau$ oscillation contour plot for 100 GeV, 2×10^{20} muons per year with 10 kT target and an angular opening of 0.1 milliradian. τ detection is through one-prong hadronic decay (see text)

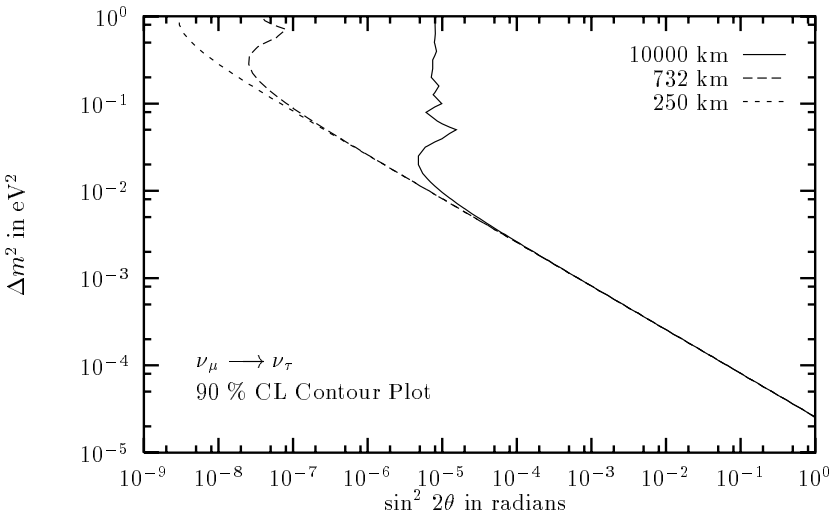

Fig. 10. 90% CL $\nu_\mu \rightarrow \nu_\tau$ oscillation contour plot for 250 GeV, 2×10^{20} muons per year with 10 kT target and an angular opening of 0.1 milliradian. τ detection is through one-prong hadronic decay (see text)

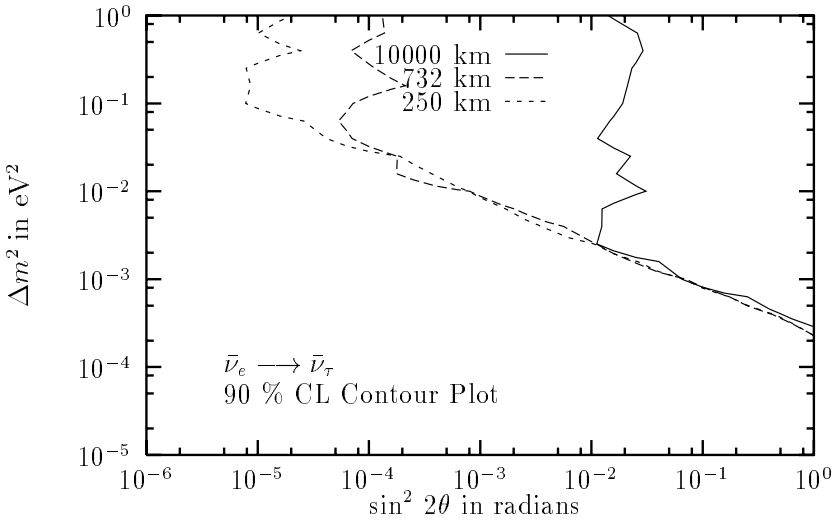

Fig. 11. 90% CL $\bar{\nu}_e \to \bar{\nu}_\tau$ oscillation contour plot for 50 GeV, 2×10^{20} muons per year with 10 kT target and an angular opening of 0.1 milliradian. τ detection through the leptonic decay mode (see text)

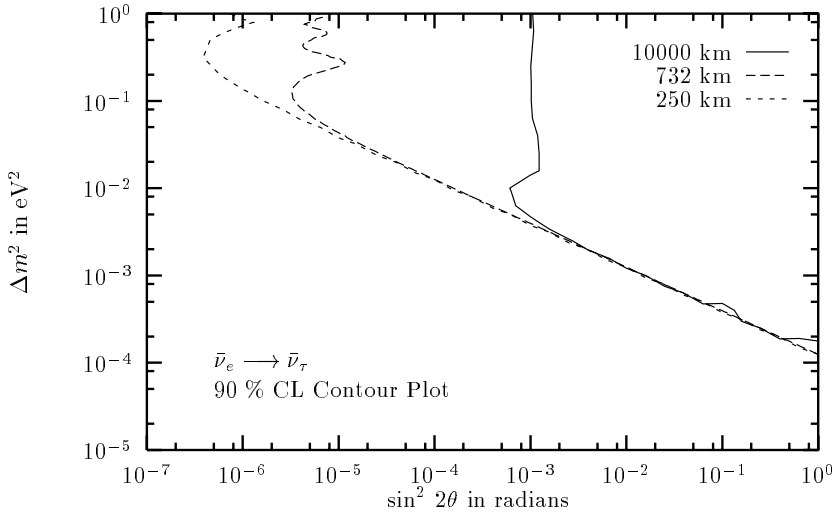

Fig. 12. 90% CL $\bar{\nu}_e \to \bar{\nu}_\tau$ oscillation contour plot for 100 GeV, 2×10^{20} muons per year with 10 kT target and an angular opening of 0.1 milliradian. τ detection through the leptonic decay mode (see text)

of energy-dependent cuts and also marginally by the fact that the plots here are for muon beam energies, while the scaling relations are for neutrino energies. It is apparent from (8) and (10) and from the contours that very long baselines offer no advantages for oscillation studies employing neutrinos from muon storage rings, and carry the added burden of impractical detector sizes, at least if conventional detectors are employed[3].

The dramatic potential for oscillation studies is apparent. Even a modest 20 GeV beam energy is capable of effectively mapping the $\nu_\mu \to \nu_\tau$ parameter space indicated by Super K, i.e. $\Delta m^2 \sim 10^{-3} - 5 \times 10^{-2}$ and $\sin^2 2\theta \sim 0.8$–1, as can be seen from Fig. 7. As expected from (10), shorter baselines provide an enhanced reach in $\sin^2 2\theta_{\min}$ ($\propto L^2$), for the same beam energy and reach in Δm^2. For $\nu_\mu \to \nu_\tau$ searches, muon storage rings enable the potential to greatly exceed the limits set by present and past accelerator experiments (NOMAD, CHORUS, CDHS, CCFR and E531) [32]. At present, bounds on this oscillation mode cover the range $\sin^2 2\theta \sim 10^{-3}$–1 and $\Delta m^2 \geq 1\,\mathrm{eV}^2$. Beam energies of 100 GeV and a baseline of 250 km would allow exploration up to $\sin^2 2\theta_{\min} \sim 10^{-7}$ and $\Delta m^2_{\min} \sim 5 \times 10^{-5}$ (Fig. 9). Similarly, the wrong sign muon mode contours (Figs. 11, 12 and 13) demonstrate the potential for extending the limits explored for $\nu_e \to \nu_\tau$ parameters. Current bounds from accelerator and reactor based experiments (NOMAD, CCFR, BUGEY and CHOOZ) [32] go down to $\Delta m^2 \geq 10^{-3}\,\mathrm{eV}^2$ and $\sin^2 2\theta \sim 5 \times 10^{-2}$–1. A 100 GeV muon beam and a 250 km baseline would extend that to $2 \times 10^{-4}\,\mathrm{eV}^2$ and 5×10^{-7}, respectively.

For convenience, in Figs. 14–17, we reproduce our contours showing how different baselines (250 km and 732 km) compare for various energies for both modes of tau appearance discussed above. The distortion of the scaling relations (8) and (10) due to the presence of experimental cuts is apparent here, being more pronounced at low beam energies. For 20 GeV and 50 GeV (Fig. 14) for instance, $\Delta m^2_{\min}$ scales as $\sim 1/E_\nu$ rather than $1/E_\nu^{1/2}$.

[3] Our motivation for focussing on medium and long baselines is in part due to the geography of existing sites where such experiments may be possible, and in part due to the fact that short baselines may require new and different detectors, which are currently under active study, as discussed in [13,31]

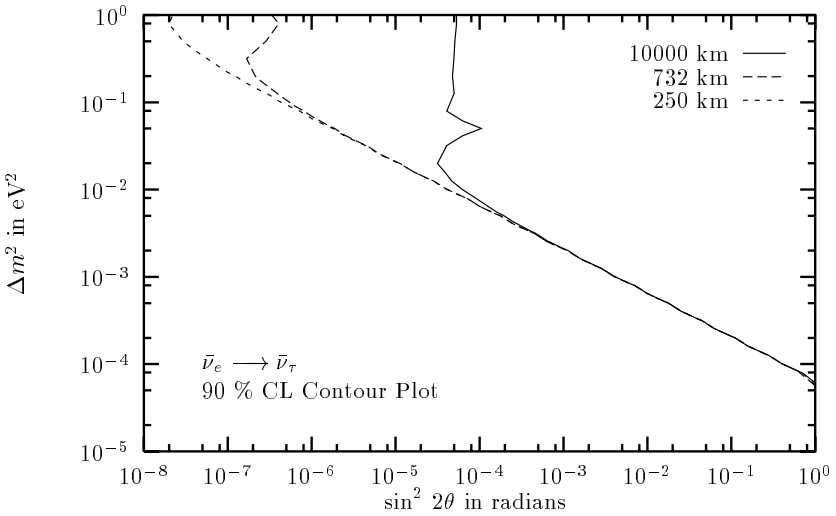

Fig. 13. 90% CL $\bar{\nu}_e \rightarrow \bar{\nu}_\tau$ oscillation contour plot for 250 GeV, 2×10^{20} muons per year with 10 kT target and an angular opening of 0.1 milliradian. τ detection through the leptonic decay mode (see text)

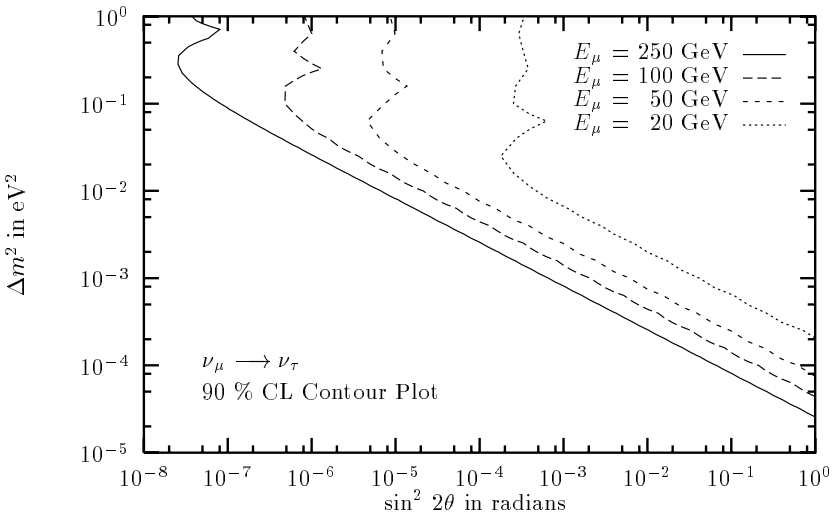

Fig. 14. 90% CL $\nu_\mu \rightarrow \nu_\tau$ oscillation contour plots for a 732 km baseline experiment, and 2×10^{20} muons per year with 10 kT target and an angular opening of 0.1 milliradian. τ detection through one-prong hadronic decay mode (see text)

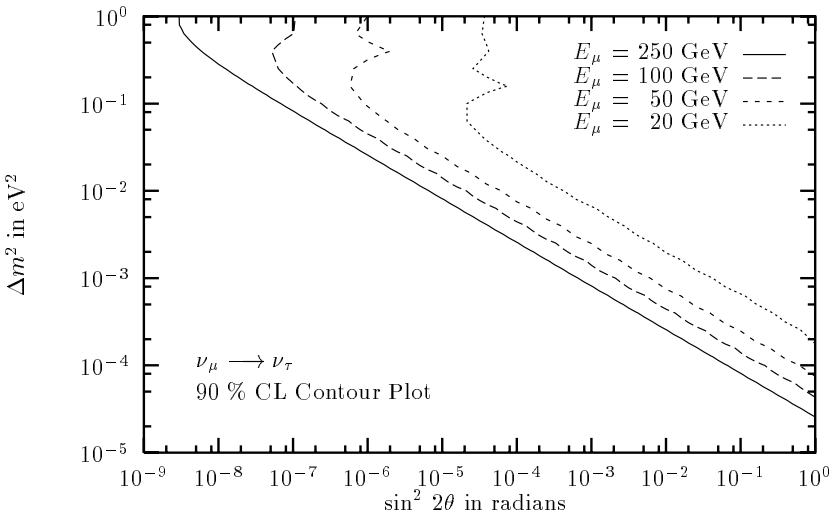

Fig. 15. 90% CL $\nu_\mu \rightarrow \nu_\tau$ oscillation contour plots for a 250 km baseline experiment, and 2×10^{20} muons per year with 10 kT target and an angular opening of 0.1 milliradian. τ detection through the one-prong hadronic decay mode (see text)

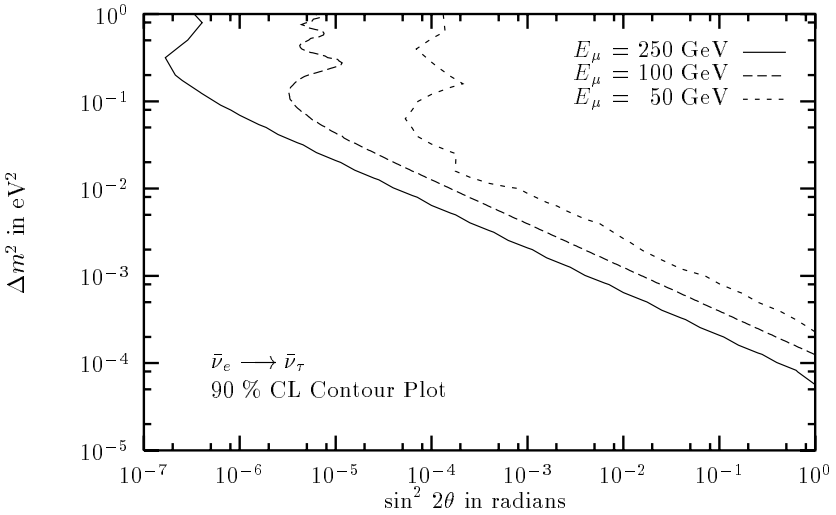

Fig. 16. 90% CL $\bar{\nu}_e \to \bar{\nu}_\tau$ oscillation contour plots for a 732 km baseline experiment, and 2×10^{20} muons per year with 10 kT target and an angular opening of 0.1 milliradian. τ detection through the leptonic decay mode (see text)

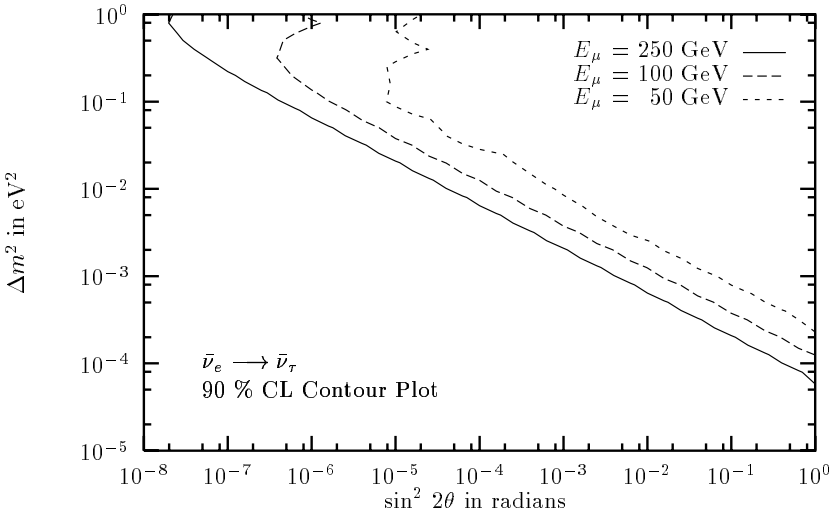

Fig. 17. 90% CL $\bar{\nu}_e \to \bar{\nu}_\tau$ oscillation contour plots for a 250 km baseline experiment, and 2×10^{20} muons per year with 10 kT target and an angular opening of 0.1 milliradian. τs are detected through leptonic decay mode (see text)

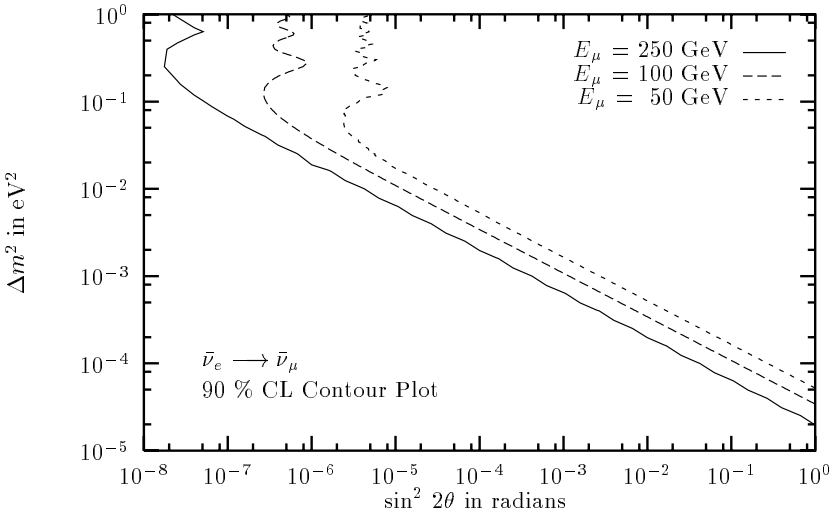

Fig. 18. 90% CL $\bar{\nu}_e \to \bar{\nu}_\mu$ oscillation contour plots for a 732 km baseline experiment, and 2×10^{20} muons per year with a 10 kT target and an angular opening of 0.1 milliradian

Finally, although our focus here has been on the detection of the ν_τ appearance, the experiments discussed here naturally lend themselves to also study $\overline{\nu_e} \to \overline{\nu_\mu}$ oscillations. The parameter regions which can be explored are shown in Fig. 18, after incorporating appropriate cuts to remove backgrounds for the wrong sign muons. Clearly, the region identified by the LSND experiment [33] can be scrutinized with ease at muon storage rings.

5 Conclusions

We have studied the possibilities offered by muon storage rings (at various muon beam energies and baselines) for ν_τ appearance experiments in order to determine masses and mixing angles for $\nu_\mu \to \nu_\tau$ and $\nu_e \to \nu_\tau$ oscillations. Tau event rates for such experiments have first been discussed with a view to understanding their variation prior to the inclusion of experimental cuts, in order to better understand how baselines, forward peaking of decay neutrinos with increasing energies, and average fluxes intercepted by detectors of various sizes can affect their optimization. Subsequently, event rates implementing cuts for hadronic and wrong sign leptonic modes are computed and used to plot contours for the parameter regions that can be explored in such experiments, and the expected scaling of the contours with energy and baseline is discussed. The results show that even for modest muon beam energies, convincing coverage and verification of the Super K parameters is possible. In addition, very significant enlargement of present day bounds on the mixing parameters for oscillations to ν_τ is guaranteed by these types of searches.

In summary, neutrinos from muon storage rings appear to be ideal sources, providing unprecedented potential for oscillation studies in the next millennium and deserve very serious consideration.

Acknowledgements. We acknowledge useful conversations with D.P. Roy, D. Choudhury and Probir Roy and also thank S. Geer and B. King for helpful exchanges over e-mail. RG would like to thank the CERN Theory Division for hospitality while this work was in progress.

References

1. Y. Fukuda et al., Phys. Lett. B **433**, 9 (1998); Phys. Rev. Lett. **81**, 1562 (1998)
2. K.S. Hirata et al., Phys. Lett. B **205**, 416 (1998); Phys. Lett. B **280**, 146 (1992); Phys. Lett. B **335**, 237 (1994)
3. D. Casper et al., Phys. Rev. Lett. **66**, 2561 (1991); R. Becker-Sendy et al., Phys. Rev. D **46**, 3270 (1992)
4. W.W.M. Allison et al., Phys. Lett. B **391**, 491 (1991); T. Kafka, Nucl. Phys. Proc. Supp. **70**, 340 (1999)
5. M. Apollonio et al., Phys. Lett. B **420**, 397 (1998)
6. G.L. Fogli, E. Lisi, A. Marrone, G. Scioscia, Phys. Rev. D **59**, 033001 (1999)
7. M. Narayan, G. Rajasekaran, S. Uma Sankar, Phys. Rev. D **58**, 031301 (1998)
8. T. Kajita, hep-ex/9810001, to appear in the proceedings of XVIII Int. Conf. on Neutrino Physics and Astrophysics (Neutrino '98), Takayama, Japan, 4–9 June 1998
9. V. Barger, Overview of Physics at a Muon Collider, Invited talk at the Fourth International Conference on the Physics Potential and Development of a Muon Collider, San Francisco, December 1997; hep-ph/9803480; V. Barger, S. Geer, K. Whisnant, Phys. Rev. D **61**, 053004 (2000)
10. J. Ellis, E. Keil, G. Rolandi, Options for Future Colliders at CERN, CERN-TH/98-033, 1998
11. C. Quigg, hep-ph/9908357
12. S. Geer, Phys. Rev. D **57**, 6989 (1998)
13. B. King, Neutrino Physics at Muon Colliders, Invited talk at the Fourth International Conference on the Physics Potential and Development of a Muon Collider, San Francisco, December 1997; BNL-65449
14. S. Geer, C. Johnstone, D. Neuffer, Muon Storage Ring Neutrino Source: The Path to a Muon Collider?, Fermilab -TM - 2073
15. A. Bueno, M. Campanelli, A. Rubbia, hep-ph/9809252
16. A Bueno, M. Campanelli, A. Rubbia, hep-ph/9808485
17. A. De Rujula, M.B. Gavela, P. Hernandez, hep-ph/9811390
18. A.M. Gago et al., hep-ph/9911470
19. D. Dooling et al., Phys. Rev. D **61**, 073011 (2000)
20. C.M. Ankenbrandt et al. (Muon Collider Collaboration), Status Report on Muon Colliders, available at http://www.cap.bnl.gov/mumu/
21. H.L. Lai et al. (CTEQ Collaboration), Phys. Rev. D **55**, 1280 (1997)
22. G. Acquistapace et al., CERN 98-02, INFN/AE-98/05, 1998
23. E. Ables et al. (MINOS Collaboration), Fermilab Proposal iP-875, 1995
24. CHORUS colaboration, E. Eskut et al., Phys. Lett. B **434**, 205 (1998); E. Pesen, Nucl. Phys. B Proc. Supp. **70**, 219 (1999)
25. NOMAD collaboration, J. Altegoer et al. CERN-EP/98-57; M. Mezzetto, Nucl. Phys. B Proc. Supp. **70**, 214 (1999)
26. F. Arneodo et al., Nucl. Phys. B Proc. Supp. **70**, 453 (1999)
27. A. Eneditato et al., Nucl. Phys. B Proc. Supp. **70**, 423 (1999)
28. B. Bullock, K. Hagiwara, A. Martin, Nucl. Phys. B **395**, 499 (1993)
29. Review of Particle Physics, Eur. Phys. J. C **3**, 21 (1998)
30. S. Raychaudhuri, D.P. Roy, Phys. Rev. D **52**, 1556 (1995); ibid., D **53**, 4902 (1996)
31. D. Harris, K. McFarland, Detectors for Neutrino Physics at the First Muon Collider, talk at the Fermilab Workshop on Physics at the First Muon Collider and at the Front End of a Muon Collider, November 1997, Fermilab CONF-98/114
32. J. Conrad, Recent Results on Neutrino Oscillations, Plenary Talk at the International Conference on High Energy Physics, Vancouver, 1998, hep-ex/9811009, and references therein
33. LSND Collaboration; C. Athanassopoulos et al., Phys. Rev. Lett. **81**, 1774 (1998)